INTERNATIONAL JOURNAL OF CONSERVATION SCIENCE

ISSN: 2067-533X Volume 7, Issue 1, January-March 2016: 57-70 www.ijcs.uaic.ro

HELLENISTIC MORTAR AND PLASTER FROM CONTRADA MELLA NEAR OPPIDO MAMERTINA (CALABRIA, ITALY)

Cristina CORTI[1*], Laura RAMPAZZI[1], Paolo VISONÀ[2]

[1] Dipartimento di Scienza e Alta Tecnologia, Università degli Studi dell'Insubria, via Valleggio 11, 22100 Como, Italy
[2] School of Art and Visual Studies, 236 Bolivar Street, University of Kentucky, Lexington, KY 40506 USA

Abstract

Recent archaeological investigations conducted at contrada Mella, an alluvial terrace near Oppido Mamertina, in southwestern Calabria, have uncovered the remains of a town that was settled by the Tauriani, an Italic people, between the third and the first centuries BC. A unique deposit excavated in 1990 and 1992 yielded numerous fragments of mortar and painted plaster associated with Hellenistic pottery and other cultural materials. Chemical analyses of samples of these fragments, point to the use of aerial mortars with hematite and calcite as pigments. The characteristics of the mortar and painted plaster found at contrada Mella are comparable to those of similar materials from Locri Epizephyrii, the closest Greek city on the Ionian coast of Italy, and from Hellenistic sites in Calabria and Sicily. They provide new evidence for interior decoration from the houses of the Tauriani.

Keywords: *Contrada Mella; Hellenistic; Tauriani; Mortar; Wall decoration*

Introduction

The ancient settlement located at contrada Mella (Strabo's Mamertion?), near Oppido Mamertina in south-western Calabria (Italy) (Fig. 1), was the main stronghold of the Tauriani, an Italic people akin to the Brettians. Built on an alluvial terrace at the foot of the Aspromonte massif, less than 20km from the Tyrrhenian coast, this hilltop town dominated the Petrace River Basin between the third and the first centuries BC. Its irregular layout included three cobblestone avenues oriented north-south and at least one east-west avenue, encompassing an area of 12 to 14 hectares. The site was destroyed (possibly during the Social War in 91-88 BC); it was partially re-occupied between the late first century BC and the late first century AD [1, 2]. Controlled excavations since 1984 have been focused upon the top and the western side of the terrace, where remains of several houses have been uncovered. In 1990 a deposit of archaeological debris was also found on the north-western slope of the terrace (Fig. 2A), within parcel 85 of Oppido Mamertina's cadastral register, at an elevation between 210 and 215m above sea level (GPS: 38º 17.59 N / 015º 57.67 E on 11.06.2012, at 1:00 PM) [3], under thick vegetation. It consisted of a large quantity of Hellenistic pottery in very good condition and other cultural materials, which were embedded in two distinctive strata of charcoaly and yellow soil overlaying a sterile light gray silty clay (Munsell: 2.5Y 7/2). It is uncertain whether this

* Corresponding author: cristina.corti@uninsubria.it

heterogeneous debris may have been an accumulation of ancient refuse or slope wash [4]. The most unusual inclusions were numerous fragments of mortar and painted plaster.

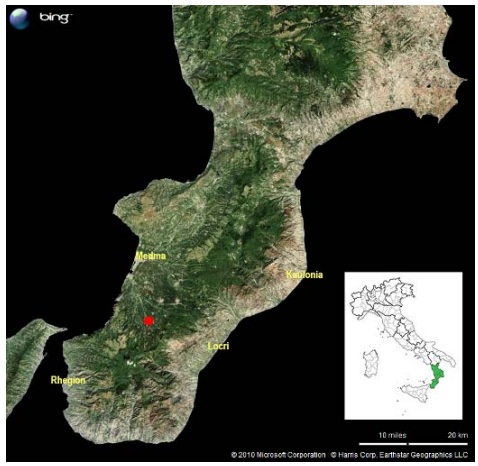

Fig. 1. Location of contrada Mella and of the nearest Greek cities in southern Calabria.
Satellite map courtesy of Bing and Microsoft Corp.
Computer-aided visualization by J.R. Jansson and L.F. Chapman

Fig. 2. a - The north-western slope of contrada Mella in 1988 and b - Area A at the end of the 1992 salvage excavation

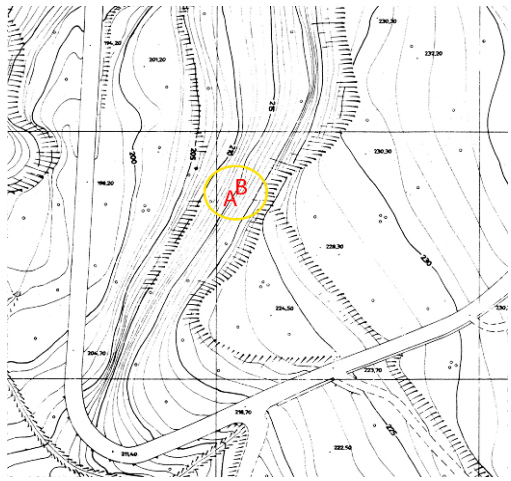

Fig. 3. Site map showing the areas (A, B) of the 1992 salvage excavations

Similar materials have occasionally been reported from Greek, indigenous, and Roman sites in Calabria [5-8]. Comparable examples are also known from Sicily and Sardinia, and from further afield [8-13, 17-18]. The entire deposit was removed in a 1992 salvage excavation of two adjacent areas, labeled A and B (Fig. 3). Most of the finds, including fineware ranging in date from the fourth to the first centuries BC and three bronze coins of Agathocles of Syracuse (c. 310-290 BC), come from area A, a 5.7m long x 1.2m wide trench (Fig. 2B). This study aims to characterize and classify the Hellenistic mortar and painted plaster from this archaeological context.

Experimental

Sampling

All the samples of bulk mortar and finishing plaster examined in this study (Table 1), totaling c. 1.75kg, come from the salvage excavations conducted in 1992. After being inventoried, they were placed in LDPE bags until their arrival at the laboratory, in order to avoid contamination.

Table 1. Description of the samples

Group	Fragment	Sample	Description
A2	A2a	A2a_m	Pinkish solid mortar
		A2a_p	Pinkish solid plaster
	A2b	A2b_m	Mortar
		A2b_p	White plaster
	A2c	A2c_m	Friable mortar
		A2c_p	White thin plaster
A3	A3a	A3a_m	Mortar
		A3a_p	White soft and friable plaster
	A3b	A3b_m	Mortar
		A3b_p	White plaster with brown stains, thin and glossy like a film
	A3c	A3c_m	Mortar
		A3c_p	Pinkish plaster
	A3d	A3d_m	Mortar
		A3d_p	Grey-orange plaster with fine-grained sand
A4	A4a	A4a_m	Mortar from 2 matching fragments
		A4a_p	Plaster from 2 matching fragments
	A4b	A4b_m	Lined mortar
		A4b_p	White plaster
A5	A5a	A5a_m	Grey-yellowish mortar (4th layer)
		A5a_p1	Red plaster (1st layer)
		A5a_p2	Pink plaster (2nd layer)
		A5a_p3	White plaster (3rd layer)
A7	A7a	A7a_m	Grey friable mortar
		A7a_p	White-grey plaster
	A7b	A7b_m	Grey mortar
		A7b_p1	Grey-yellowish film
		A7b_p2	White layer under the grey-yellowish film
	A7c	A7c_m	Mortar
		A7c_p	White plaster with cracks
A9	A9a	A9a_m	Very friable mortar
		A9a_p	Pinkish solid plaster
A15	A15a	A15a_m	White mortar
		A15a_p	Pink plaster
	A15b	A15bc_m	Yellowish mortar under A15b_p and A15c_p
		A15b_p	Yellowish plaster
		A15c_p	White plaster
	A15d	A15d_m	Mortar
		A15d_p	Pink plaster
A22	A22a	A22a	Smooth fragment
	A22b	A22b_m	“Chocolate-brown” spongy mortar
B2	B2	B2_m	White mortar
		B2_p	White plaster

The samples were then carefully sorted, in order to identify the peculiar features of each of them and to separate out those that were potentially more informative. Subsequently, they were dry-cleaned and the dirt with which they were covered was removed with a soft brush. Lastly, they were photographed, catalogued, and stored in LDPE vials or bags, until the time of analysis.

The samples were labeled according to the pottery bucket system used by the archaeologists: capital letter and number, A2, A3, etc., followed by a lowercase letter that identifies each fragment (a, b, c, etc.) and by the initials m and p (for bulk mortar and finishing plaster, respectively). Mortars came from the "bulk layer" of the samples and consisted of a lime binder and a coarse aggregate. The finishing layers of the samples were classified as "plasters"; this particular kind of mortars was prepared with a lime binder and a finer aggregate, and it was smoothed at the surface.

Since FTIR, TG-DSC and XRD techniques require pulverized samples, a small fraction was taken from each sample that would be representative of the entire fragment. This subsequently was ground in an agate mortar or by means of a steel ball mill, in order to obtain a fine and homogeneous powder.

Samples for SEM-EDX were analyzed both without any pre-treatment and in polished cross sections.

X-ray powder diffraction analysis

X-ray diffraction analyses were conducted using a Bruker AXS D8 ADVANCE diffractometer (30kV, 40mA, Cu-Kα radiation (λ=1.5418Å), graphite monochromator, 5-55° 2θ, step scan Δ2θ = 0.02°, counting time t = 1s) and a Rigaku Miniflex 300 (30kV, 10mA, Cu-Kα radiation (λ=1.5418Å), 5-55° Theta/2-Theta, step scan 0.02°, scan speed 3°/min). DIFFRACplus EVA and PDXL2 softwares and paper-based databases were used to identify the mineral phases in each X-ray powder spectrum, by comparing experimental peaks with reference patterns. The semi-quantitative mineralogical composition of each sample was also calculated.

Thermal Analysis

Thermal analysis (TGA/DSC) was performed by means of a NETZSCH STA 409 PC instrument. Samples were placed in aluminum crucibles, with the temperature program ranging from room temperature to 900°C, at a heating rate of 10°C min^{-1} under pure nitrogen atmosphere. TG and DSC raw data were corrected on the basis of a background curve.

Fourier Transform Infrared Spectroscopy

FTIR spectra were recorded on KBr pellets (Sigma-Aldrich FTIR Grade) in transmission mode, by a BioRad Excalibur Series FTS 3000 spectrometer (detector DTGS) in the 4000–400cm^{-1} range, with a resolution of 4cm^{-1}.

Pellets were prepared by mixing samples and KBr in an agate mortar, pouring the mixture into a press and then applying a pressure of 6t/cm^2 for 1 minute.

Paper-based databases were used to identify the species in each FTIR spectrum, by comparing experimental peaks with reference patterns.

Scanning Electron Microscopy and Energy Dispersive X-ray spectroscopy

The morphology of a selection of samples was observed with a FEI/Philips XL30 ESEM. The elemental analyses were carried out using an X-ray energy dispersive spectrometer EDX Quantax 400 coupled to SEM.

Every sample was analyzed "as is" in low vacuum mode (1torr) at 20kV, by using GSE, BSE and X-Ray detectors.

A selection of samples was embedded in an epoxy resin, cross-cut with a diamond saw and then mechanically polished. Polished cross sections were then observed with SEM-EDX using the same methodology described above.

Optical microscopy

Polished cross sections were observed using an optical microscope Nikon Eclipse LV150, equipped with a Nikon DS-FI1 digital image acquisition system. Images were acquired and elaborated using the NIS-elements F software.

Results and Discussions

Most of the samples showed a "bulk layer" (referred to as "mortar" in this work), consisting of lime binder and coarse aggregate, and a single finishing layer (referred to as "plaster"), of variable thickness, composed of a different mortar, with lime binder and a finer aggregate, refined and smoothed at the surface [13]. In some cases, the aggregate could not even be seen with an optical microscope. The sample A5 (Fig. 4C) was a notable exception, as it showed the presence of three colored layers (white, pink and red) above the coarse mortar. Other samples with more than one layer of plaster were A2b, A3c, A7b and A15b, even if the sequence of the layers was often irregular or poorly defined. Worth noting was the apparent presence of *cocciopesto* in the sample A2a, both in the mortar and in the plaster. Sample A3b (Fig. 4) showed a layer of mortar and a layer of white hard plaster, with brown spots perhaps due to another superimposed layer, above which, in some points, a glossy film seemed to be present. Finally, two fragments, A4a (Figure 4B) and A7c (Fig. 4D), had grooves similar to those mentioned by Bonturi et al. [6], which may have been scored on the plaster while it was still wet to facilitate the adhesion of a subsequent layer. However, the possibility that these grooves had a decorative function, like those on some of the Hellenistic plaster from the "casa dei leoni" at Locri Epizephyrii [5], cannot be ruled out.

Fig. 4. The samples: a - A3b, b - A4a, c - A5, d - A7c

FTIR

FTIR analysis allowed determining the qualitative composition of the samples under examination. The results are presented in Table 2.

FTIR analyses revealed the presence of carbonates in all the samples. Carbonates were identified by means of their characteristic bands in the 1440-1430cm^{-1} range, bound to the asymmetric stretching of C-O. The peaks at 874 (out-of-plane bending vibration), 713 (in-plane

bending vibration), 1798 and 2514cm^{-1} (combination modes) led us to identify these carbonates as calcite [$CaCO_3$].

In some samples (A2c_m, A4a_p, A7b_m, A15bc_m, A15c_p, B2_p), it is possible to find another peak at about 858cm^{-1} (out-of-plane bending vibration), which indicates the presence of aragonite, the metastable orthorhombic form of calcium carbonate, less common than calcite.

Almost all the samples show bands in the ranges 1200-900 and 500-400cm^{-1}, generally coming from the vibrations of SiO_4 group of silicates. Specifically, quartz [SiO_2] can be identified from the presence of a peak at 1080cm^{-1} and from its peculiar doublet at about 780 and 795cm^{-1}.

All samples show peaks around 2870-2980cm^{-1}, characteristic of the stretching of the C-H groups; many of them also display bands in the regions around 1630cm^{-1} or 1230cm^{-1}, thus suggesting the presence of organic substances, but the amount was too small for a reliable identification [14]. See, e.g., in Figure 5, the FTIR spectrum of sample A4a_p. Peaks of calcite, aragonite, quartz and silicates are noticeable.

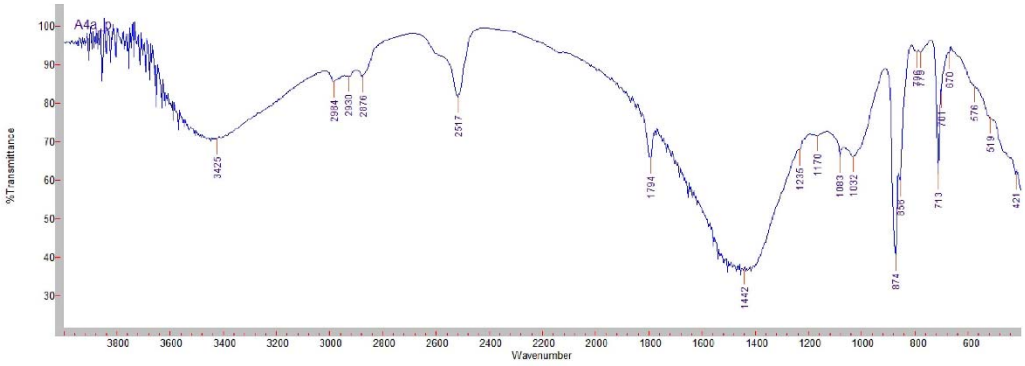

Fig, 5. FTIR transmission spectrum of sample A4a_p in KBr. Peaks of calcite (2517, 1794, 1442, 874, 713cm^{-1}), aragonite (856cm^{-1}), quartz (1083, 796, 779cm^{-1}), silicates (1032, 576, 519, 421cm^{-1}), organic substances (2984, 2930, 2876, 1235cm^{-1}) are noticeable

XRD

All the samples were analyzed by X-ray diffraction (XRD). The results are reported in Table 3.

With regards to carbonates, XRD analyses showed the presence of abundant calcite [$CaCO_3$] or magnesian calcite [$(Ca,Mg)CO_3$] in all the samples, as expected [11]. Traces of aragonite [$CaCO_3$] were found in samples A4a_p, A3a_p, and B2_p, all of which were fragments of white (or whitish) plasters.

Dolomite [$MgCa(CO_3)_2$] was found in two samples of mortars (A3b_m and A22b_m).

Quartz [SiO_2], generally very abundant, was found in all the samples.

Feldspars (albite [$NaAlSi_3O_8$], anorthite [$CaAl_2Si_2O_8$], and anorthoclase [$(Na,K)AlSi_3O_8$]) are also widespread, since they were found in all but three samples of plasters from the A7 group.

Phyllosilicates, generally muscovite [$KAl_3Si_3O_{10}(OH,F)_2$], were found in a large number of samples, both plasters and mortars.

Of particular interest is the presence of hematite, found in small quantities in four samples of pink plasters and in the only sample of red plaster [11]. Hematite was identified by means of its characteristic peak at d = 2.70Å [15]. One can see that some results are slightly different from those obtained from FTIR analysis, e.g. in regards to aragonite: this may be due

to the different sensitivity of the two techniques, or to some problem related to overlapping peaks.

Table 2. FTIR transmission results

Group	Fragment	Sample	Calcite	Aragonite	Quartz	Silicates	Organic compounds
A2	A2a	A2a_m	*		*	*	*
		A2a_p	*		*	*	*
	A2b	A2b_m	*		*	*	*
		A2b_p	*		*	*	*
	A2c	A2c_m	*	*	*	*	*
		A2c_p	*		*	*	*
A3	A3a	A3a_m	*		*	*	*
		A3a_p	*		*	*	*
	A3b	A3b_m	*		*	*	*
		A3b_p	*		*	*	*
	A3c	A3c_m	*		*	*	*
		A3c_p	*		*	*	*
	A3d	A3d_m	*		*	*	*
		A3d_p	*		*	*	*
A4	A4a	A4a_m	*		*	*	*
		A4a_p	*	*	*	*	*
	A4b	A4b_m	*		*	*	*
		A4b_p	*		*	*	*
A5	A5a	A5a_m	*		*	*	*
		A5a_p1	*		*	*	*
		A5a_p2	*		*	*	*
		A5a_p3	*		*	*	*
A7	A7a	A7a_m	*		*	*	*
		A7a_p	*		*	*	*
	A7b	A7b_m	*	*	*	*	*
		A7b_p1	*			*	*
		A7b_p2	*		*	*	*
	A7c	A7c_m	*		*	*	*
		A7c_p	*		*	*	*
A9	A9a	A9a_m	*		*	*	*
		A9a_p	*		*	*	*
A15	A15a	A15a_m	*		*	*	*
		A15a_p	*		*	*	*
	A15b	A15bc_m	*	*	*	*	*
		A15b_p	*		*	*	*
	A15c	A15bc_m	*	*	*	*	*
		A15c_p	*	*	*	*	*
	A15d	A15d_m	*		*	*	*
		A15d_p	*		*	*	*
A22	A22a	A22a	*		*	*	*
	A22b	A22b_m	*		*	*	*
B2	B2	B2_m	*		*	*	*
		B2_p	*	*	*	*	*

TG-DSC

TG-DSC analysis of mortars is useful to highlight the quantity and composition of the binder, making it also possible to detect the nature of the compounds constituting the hydraulic binder that are often not perfectly crystallized, and are therefore difficult to identify by other techniques such as XRD. TG-DSC allowed us to compute the percentage of calcite present in the samples investigated.

Table 3. XRD semiquantitative analysis data

Group	Fragment	Sample	Calcite	Aragonite	Magnesian calcite	Dolomite	Quartz	Feldspars	Phyllosilicates	Hematite	Other
A2	A2a	A2a_m	+++				+++	++	+	+/-	
		A2a_p	+++				+++	++	+		
	A2b	A2b_m	+++				+++	++	+/-		
		A2b_p			+++		++	+			
	A2c	A2c_m			+++		++	++			
		A2c_p	+++				+	+			
A3	A3a	A3a_m			+++		+++	++			
		A3a_p		+/-	+++		++	+			
	A3b	A3b_m			+++	++	+	+/-			
		A3b_p	+++				+/-	+			
	A3c	A3c_m			+++		+++	+++			
		A3c_p	+++				+	+/-	+/-		
	A3d	A3d_m			+++		++	+++	+/-		
		A3d_p			+++		+++	++	+/-		
A4	A4a	A4a_m	++				+++	++	+		
		A4a_p	+++	+			++	+			
	A4b	A4b_m			++		+++	+			
		A4b_p	+++				++	+			++
A5	A5a	A5a_m			+++		++	+++	+		
		A5a_p1	+++				+++	++	+	+	
		A5a_p2	+++				+++	+++	+	+/-	
		A5a_p3	+++				++	+	+/-		
A7	A7a	A7a_m	+++				+++	++	+/-		
		A7a_p	+++				+++	+++	+/-		
	A7b	A7b_m			+++		+++	+++			
		A7b_p1	+++				+				
		A7b_p2			+++		++		+/-		
	A7c	A7c_m			+++		+	+++	+/-		
		A7c_p	+++				+/-				
A9	A9a	A9a_m			++		+++	+	+		
		A9a_p	+++				+++	+	+/-	+/-	
A15	A15a	A15a_m			++		+++	++	+		
		A15a_p	+++				+++	++	+		
	A15b	A15bc_m	+++				+++	++	+		
		A15b_p	+++				++	+			
	A15c	A15bc_m	+++				+++	++	+		
		A15c_p	+++				+++	++	+/-		
	A15d	A15d_m	++				+++	++	+		
		A15d_p	+++				+++	+	+/-	+	
A22	A22a	A22a	+++				+++	+	+/-		
	A22b	A22b_m			+++	++	++	+/-			
B2	B2	B2_m	+++				+++	+++	+/-		+/-
		B2_p	+++	+			++	+			

Legend: +++ very abundant (>40%); ++ abundant (15-40%); + present (3-15%); +/- scarce (<3%)

When the carbonate component is completely and exclusively attributable to the binder, it is possible to calculate the ratio of binder/aggregate, which provides fundamental information on the production technology of the mortars.

An examination of the geological map of the region of Oppido Mamertina points to the presence of gneiss outcrops, producing a quartz-silicate sand, typical of the small streams near Oppido. This region is also characterized by Pliocenic sediments, such as clayey fossiliferous sands, blue fossiliferous clays, crystalline conglomerates, white marls with foraminifera. Fossiliferous sands contain a carbonate fraction due to the shells of fossil.

On the basis of these considerations, of preliminary data from an archaeological site closely related to contrada Mella [16], and of the results of XRD analysis that found some evidence of aragonite in some samples, the presence of a small carbonate fraction in the aggregate cannot be ruled out. This could lead to an overestimation of the binder, as calculated by TG analysis.

As the analyzed mortars are coeval and come from the same site, it can be inferred that their raw materials came from the same areas and that this overestimation applies to all the samples. To use this technique for a comparison and a classification of the different mortars is, in our opinion, still valid.

The coefficient of hydraulicity of the mortar, defined as the ratio between the percentage of CO_2, lost above 600°C, and the percentage of water bound to hydraulic compounds, lost between 200 and 600°C, was also calculated. These coefficients are defined by these relevant ranges of temperature [17-21]:

- <120°C loss of hygroscopic water;
- 120-200°C dehydration of gypsum and salt hydrates;
- 200°-600°C loss of water bound to hydraulic components;
- 600°C decomposition of calcite and other carbonates.

TG-DSC analysis was conducted on a selection of 17 samples, chosen in order to be representative of all the typologies. As had already been found from FTIR and XRD analysis, all samples contain calcium carbonates, losing CO_2 above 600°C; almost all samples exhibit a single peak in DTG (thermogravimetric derivative curve) around 700-750°C. The samples A3d_m and A15c_p show a second peak at a temperature above 800°C: the presence of less pure forms of calcite could be assumed.

Samples containing quartz have a characteristic endothermic peak at about 570°C in the DSC plot, due to a transition between two crystalline phases: the results show that all the samples contain quartz, except for the samples A3b_p, A3c_p, A7c_p (quartz poor in FTIR and XRD) and A7b_p1 (quartz absent in FTIR, poor in XRD).

Finally, some samples exhibit weight losses in the region between 400 and 450°C that could be related to the presence of organic matter. This can be noted, in particular, in the samples A3d_p, A4b_p and in the group of three plasters of the fragment A5 (A5a_p1, A5a_p2, A5a_p3); for some of these, the possible presence of organic compounds was also highlighted by FTIR analysis. The data relating to calcite %, binder/aggregate ratio and coefficient of hydraulicity can be represented graphically for clarity.

The graph of calcite % vs. the group (A3, A4, etc.) is shown in Figure 6A. A glance at this figure reveals that sample A7b_p1 is clearly distinctive. This sample consists of a sort of film overlying the plaster layer. Furthermore, in nearly all cases, plaster samples are richer in calcite than mortar ones.

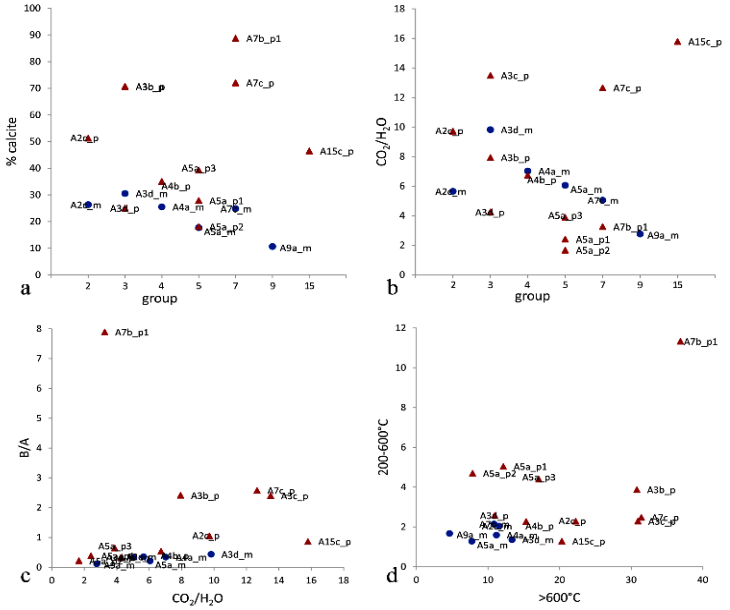

Fig. 6. a - % calcite relative to the different groups, b - hydraulicity coefficient relative to the different groups, c - B/A ratio vs. hydraulicity index, relative to the different groups, d - Loss of weight between 200-600°C vs. above 600°C, relative to the different groups. In all the four graphs, circles correspond to mortars and triangles to plasters

In addition, as far as the hydraulicity coefficient is concerned, it can be noted that there are no particular differences between plasters and mortars, although the samples that have higher aerial characteristics are still those of plaster (Fig. 6B).

Observing the graph representing the binder/aggregate ratio vs. the hydraulicity coefficient (Fig. 6C), with samples grouped by type (plaster or mortar), it can be noticed that mortar samples cluster at low B/A ratios and low hydraulicity coefficients, whereas plaster samples show less homogeneous results. The different groups of samples (A3, A4...) do not show significant groupings, except for the two A4 samples and for the three different fragments of plaster of sample A5.

The last graph (Fig. 6D) shows the amount of water (%) lost between 200 and 600°C vs. the amount of carbon dioxide (%) lost above 600°C, with the indication of the type of the samples. It is possible to note the grouping of mortar samples, which appear more homogeneous than those of plaster. As regards the different groups, no particular trends can be noted, apart from the plasters coming from group A5. Sample A7b_p1 confirms its peculiarity among all the samples that have been analyzed.

SEM-EDX and Optical microscopy

Some representative samples were observed by means of SEM-EDX, both without pre-treatment and in polished cross sections. Sample A5, with its red plaster (Fig. 7), was particularly interesting. In Figure 8A a global view in backscattered electrons of the surface of this plaster can be seen. In Figure 8B, a magnified view of some "bright" particles can be appreciated. As can be seen from their EDX spectra (Figure 8C and Figure 8D), these particles are particularly rich in Fe if compared with the mean spectrum of the total area. A semiquantitative analysis gave estimation that the content in Fe equals about 30% w/w for the particles, versus 8% w/w for the total area. Similarly, other "bright" particles showed content in Fe (% w/w) between 40-45%, versus a mean content in the total analyzed area lower than 5%. These data confirmed the presence of a pigment rich in iron, diffused in the plaster in the form of particles of irregular dimensions, as can be seen even in Figure 9, where a SEM-EDX analysis of the cross section of this sample can be seen. The elemental map shows clearly the general presence of diffuse iron and of some coarser particle rich in this element. On the basis of the results of XRD analysis, this pigment can then be identified as hematite [11].

Fig. 7. Optical microscopy image of the red plaster of sample A5 in polished cross section (bar=0.5mm)

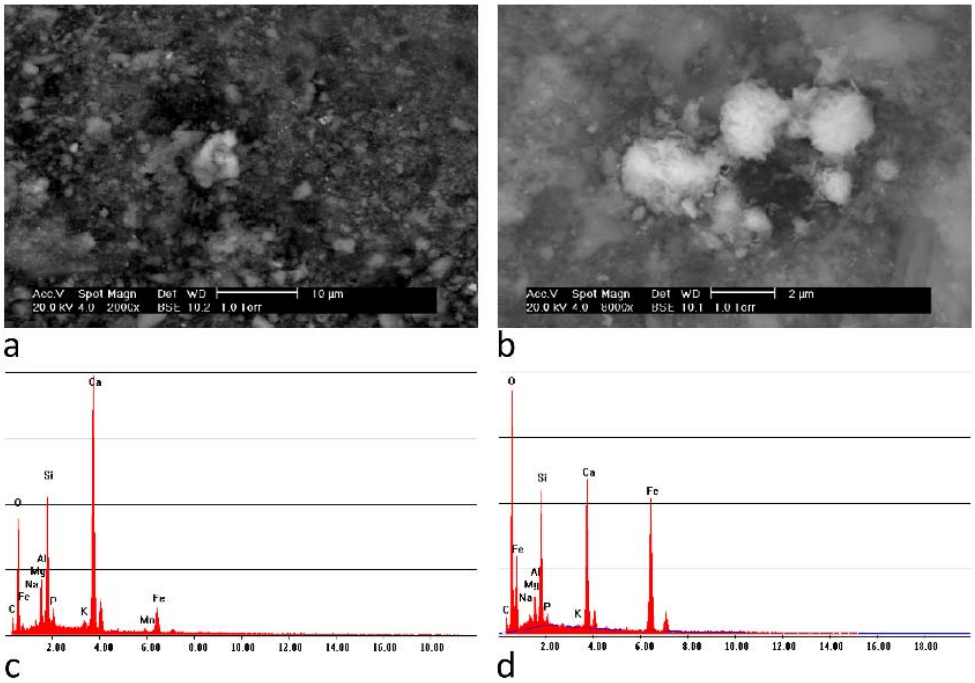

Fig. 8. SEM image and EDX spectrum of sample A5: a - area of the surface of red plaster, b - bright particles on the surface of the red plaster, c - EDX spectrum of an area on the surface of the red plaster and d - EDX spectrum of bright particles on the surface of the red plaster

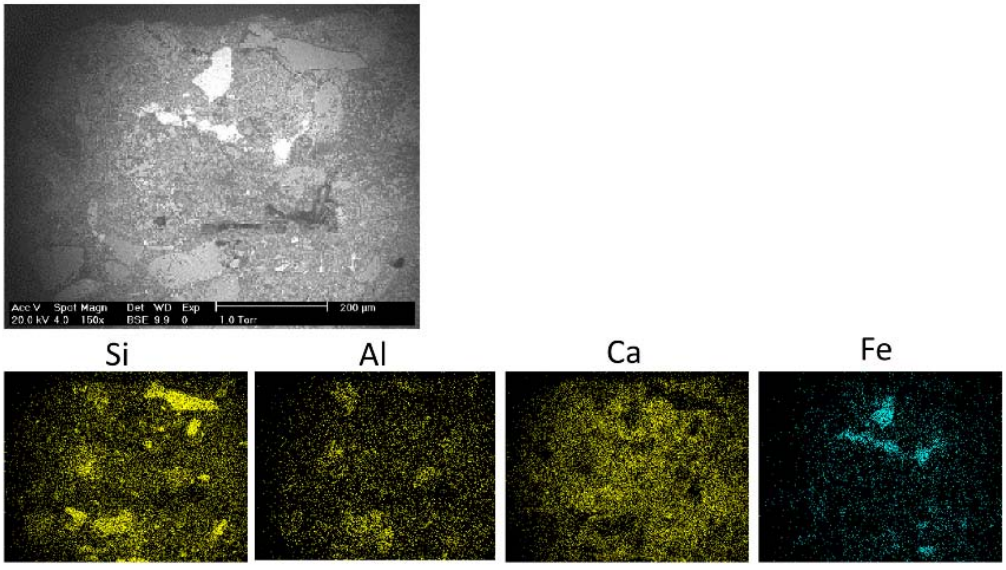

Fig. 9. EDX maps of a polished cross section of the red plaster on Sample A5

One can see in Figure 9 that iron is diffused in a matrix of calcium and is particular abundant in regions corresponding to coarser bright particles

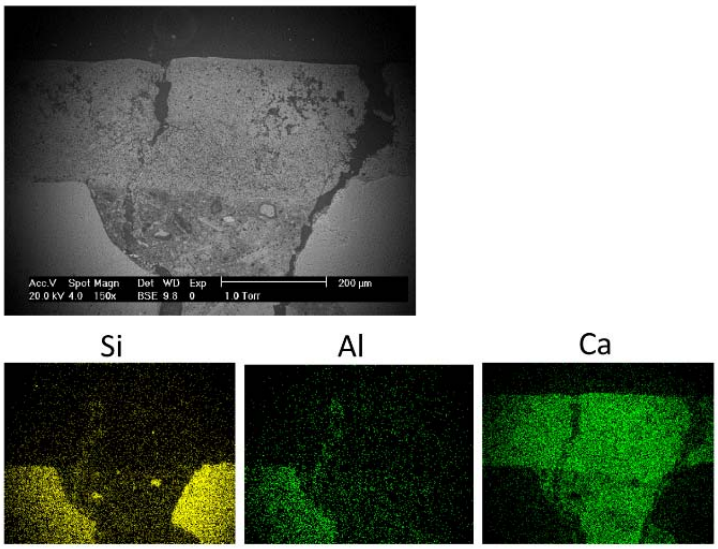

Fig. 10. EDX maps of a polished cross section on sample A3b

It also can be seen in figure 10 that the bulk mortar is constituted by a Ca-rich binder and a coarse Si-Al aggregate. As far as plaster is concerned, it is composed of a binder rich in Ca and a very fine aggregate.

SEM-EDX analysis of cross sections determined that mortars consist of a calcitic binder and an irregular aggregate. While the coarser fractions mostly consist of silico- and silico-aluminate particles (Figure 10), the presence of carbonate particles in the finer fraction of aggregate cannot be ruled out. The finishing plasters, on the other hand, are generally more homogenous than bulk mortars, with a calcium binder and a finer aggregate.

Conclusions

This study seeks to characterize and classify samples of mortars and painted plasters from the Italic town of contrada Mella which attest to the local use of these materials in the Hellenistic period. Examples of plaster with similar colors are known from contemporary Greek and indigenous sites in Calabria and Sicily [7, 11, 12, 22]. An examination of select fragments has revealed the presence, in most cases, of a bulk layer ("mortar") consisting of lime and coarse aggregate and a single layer of plaster, with a finer aggregate and a smooth surface. In all the samples the aggregate fraction contained quartz and other silicates, usually phyllosilicates and feldspars. The identification of a natural pigment made of hematite in four samples of pink plasters and in the only sample of red plaster is especially noteworthy. The finding of hematite points to the use of a natural ochre, the cheapest and most widespread red pigment [5, 23]. For the most part, the samples of plaster were richer in calcite compared to the corresponding mortars, as confirmed by the standard "formulas" of preparation. Since mortar or plaster has rarely been found in excavations at contrada Mella, and mostly in granular form (possibly because of the high acidity of the soil), this unique trove suggests that some houses of the Tauriani may have had patterns of wall decoration similar to those found elsewhere in Magna Graecia and Sicily.

Acknowledgments

The authors are grateful to Elena Lattanzi, former Archaeological Superintendent of Calabria, and to the Soprintendenza per i Beni Archeologici della Calabria, for generously

allowing the analysis of select specimens of mortar and plaster from the excavations at contrada Mella in 1992. Lesley F. Chapman (Visual Resources Curator, Department of Art and Art History, Colgate University, Hamilton, NY, USA), James R. Jansson (The Foundation for Calabrian Archaeology, Parker, CO, USA), Jennifer E. Knapp (Langara College, Vancouver, BC, Canada), Ryan Hagan (University of Kentucky), Roberto Bugini (ICVBC-CNR, Milan, Italy) and Daniela Mastricchio also contributed to this essay.

We heartily acknowledge the Fondazione Banca del Monte di Lombardia for partial financial support.

References

[1] L. Costamagna, P. Visonà, **Oppido Mamertina: Calabria, Italia: ricerche archeologiche nel territorio e in contrada Mella**, Gangemi, Roma, 1999.

[2] R. Agostino, *L'abitato brettio di Mella*, **Il territorio di Oppido Mamertina dall'antichità all'età contemporanea., Sila Silva ho drumós… hón Sílan kaloûsin. Conoscenza e recupero nel Parco Nazionale d'Aspromonte** (Editor: R. Agostino), Rubettino, Soveria Mannelli, 2009, pp. 61-74.

[3] L. Costamagna, *Il terrazzo di Oppido Vecchio e l'insediamento di Mella: il quadro topografico*, **Oppido Mamertina: Calabria, Italia: ricerche archeologiche nel territorio e in contrada Mella** (Editors: L. Costamagna and P. Visonà), Gangemi, Roma, 1999, pp. 177-183.

[4] J.E. Knapp, *Shaping identity: an analysis of Hellenistic Southern Italian ceramics and its implications for cultural and societal change*, **PhD Thesis**, University of Missouri-Columbia, 2014.

[5] M. Rubinich, *I rivestimenti di intonaco*, **Locri Epizefiri, IV. Lo Scavo di Marasà Sud, il Sacello Tardo-Arcaico e la "Casa dei Leoni"** (Editor: M. Barra Bagnasco), Le lettere, Firenze, 1992, pp. 303-317.

[6] M. Bonturi, V. Centol, *Considerazioni preliminari sugli intonaci rinvenuti presso il lato orientale del tempio C, ambiente A*, **Grumento e il suo territorio nell'antichità** (Editor: A. Mastrocinque), Archaeopress, Oxford, 2013, pp. 97-101.

[7] D. Falcone, **Domátia: case d'età greca in Calabria**, Laruffa, Reggio Calabria, 2009.

[8] I. Cardoso, M. Macedo, F. Vermeulen, C. Corsi, A. Santos Silva, L. Rosado, A. Candeias, J. Mira, *A multidisciplinary approach to the study of archaeological mortars from the town of Ammaia in the Roman Province of Lusitania (Portugal),* **Archaeometry, 56**, 2014, pp. 1-24.

[9] A. Toscano Raffa, *Gli apparati decorativi delle case del periodo II*, **Finziade I. Gli scavi sul Monte Sant'Angelo di Licata (2003-2005)** (Editors: G.F. La Torre and F. Mollo), Giorgio Bretschneider, Roma, 2013, pp. 214-223.

[10] I. Colpo, *I frammenti di intonaco e di stucco modanato*, **Nora. Il Foro Romano. Storia di un'area urbana dall'età Fenicia alla tarda antichità, 1997-2006** (Editors: J. Bonetto, A.R. Ghiotto, M. Novello and G. Falezza), Università degli studi di Padova. Dipartimento di archeologia, Padova, 2009, pp. 777-782.

[11] G. Barone, V. Crupi, C. Ingoglia, D. Majolino, P. Mazzoleni, V. Venu, *Il contributo dell'archeometria allo studio della pittura in Sicilia: il progetto su Licata (relazione preliminare)*, **Pittura Ellenistica in Italia e in Sicilia. Atti del Convegno di Studi** (Editors: G.F. La Torre and M. Torelli)**,** Messina, 24-25 settembre 2009, 2011, pp. 241-254.

[12] G.F. La Torre, *Origine e sviluppo dei sistemi di decorazione parietale nella Sicilia ellenistica*, **Pittura Ellenistica in Italia e in Sicilia. Atti del Convegno di studi** (Editors: G.F. La Torre and M. Torelli)**,** Messina, 24-25 settembre 2009, 2011, pp. 255-277.

[13] I. Garofano, M. Robador, A. Duran, *Materials characteristics of Roman and Arabic mortars and stuccoes from the Patio de Banderas in the Real Alcazar of Seville (Spain),* **Archaeometry, 56**, 2014, pp. 541-561.
[14] M. Stefanidou, I. Papayianni, V. Pachta, *Evaluation of inclusions in mortars of different historical periods from Greek monuments,* **Archaeometry, 54,** 2012, pp. 737-751.
[15] A. Duran, M. Jimenez De Haro, J. Perez-Rodriguez, M. Franquelo, L. Herrera, A. Justo, *Determination of pigments and binders in Pompeian wall paintings using synchrotron radiation - high resolution x-ray powder diffraction and conventional spectroscopy – chromatography,* **Archaeometry, 52**, 2010, pp. 286-307.
[16] R. Agostino, G. Barone, P. Mazzoleni, S. Raneri, G. Sabatino, M.M. Sica, *Mortars and plasters from the Bruttii-Roman city of Taureana (Palmi, RC, Italy)-preliminary data*, **Periodico di Mineralogia, 82**, 2014, pp. 489-501.
[17] G.M. Ingo, I. Fragala, G. Bultrini, T. De Caro, C. Riccucci, G. Chiozzini, *Thermal and microchemical investigation of Phoenician-Punic mortars used for lining cisterns at Tharros (western Sardinia, Italy),* **Thermochimica Acta, 418**, 2004, pp. 53-60.
[18] C. Genestar, C. Pons, A. Mans, *Analytical characterisation of ancient mortars from the archaeological Roman city of Pollentia (Balearic Islands, Spain),* **Analytica Chimica Acta, 557**, 2006, pp. 373-379.
[19] A. Moropoulou, A. Bakolas, K. Bisbikou, *Characterization of ancient, Byzantine and later historic mortars by thermal and X-ray diffraction techniques,* **Thermochimica Acta, 269,** 1995, pp. 779-795.
[20] A. Bakolas, G. Biscontin, A. Moropoulou, E. Zendri, Characterization *of structural byzantine mortars by thermogravimetric analysis,* **Thermochimica Acta, 321,** 1998, pp. 151-160.
[21] W. Bartz, T. Filar, *Mineralogical characterization of rendering mortars from decorative details of a baroque building in Kozuchow (SW Poland),* **Materials Characterization, 61**, 2010, pp. 105-115.
[22] R.C. Westgate, *Space and decoration in Hellenistic houses,* **The Annual of the British School at Athens, 95**, 2000, pp. 391-426.
[23] E. Gliozzo, F. Cavari, D. Damiani, I. Memmi, *Pigments and plasters from the Roman settlement of Thamusida (Rabat, Morocco),* **Archaeometry, 54,** 2012, pp. 278-293.

Received: June, 04, 2015
Accepted: February, 02, 2016